

A method for in situ absolute DD yield calibration of neutron time-of-flight detectors on OMEGA using CR-39-based proton detectors

C. J. Waugh, M. J. Rosenberg, A. B. Zylstra, J. A. Frenje, F. H. Séguin, R. D. Petrasso, V. Yu. Glebov, T. C. Sangster, and C. Stoeckl

Citation: [Review of Scientific Instruments](#) **86**, 053506 (2015); doi: 10.1063/1.4919290

View online: <http://dx.doi.org/10.1063/1.4919290>

View Table of Contents: <http://scitation.aip.org/content/aip/journal/rsi/86/5?ver=pdfcov>

Published by the [AIP Publishing](#)

Articles you may be interested in

[A technique for verifying the input response function of neutron time-of-flight scintillation detectors using cosmic rays](#)

Rev. Sci. Instrum. **85**, 11D633 (2014); 10.1063/1.4896958

[A new neutron time-of-flight detector for fuel-area-density measurements on OMEGA](#)

Rev. Sci. Instrum. **85**, 11E102 (2014); 10.1063/1.4886428

[The response of CR-39 nuclear track detector to 1–9 MeV protons](#)

Rev. Sci. Instrum. **82**, 103303 (2011); 10.1063/1.3653549

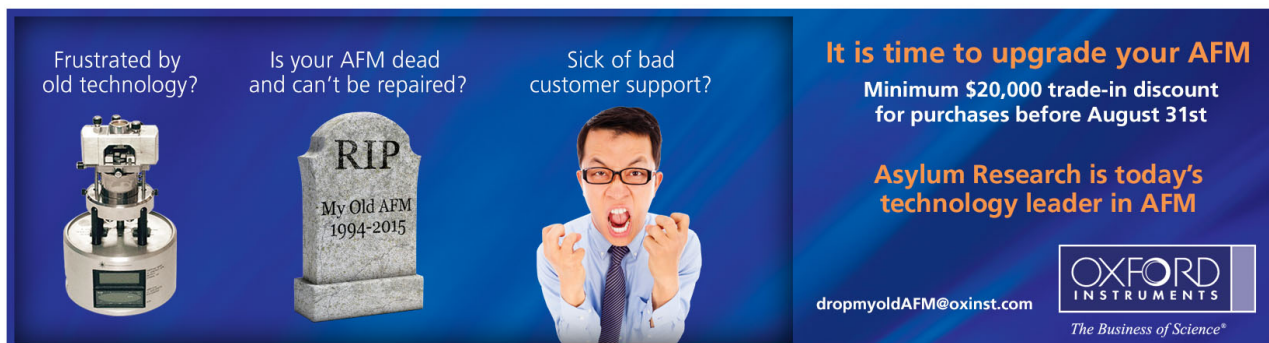
[Absolute calibration of photostimulable image plate detectors used as \(0.5 – 20 MeV \) high-energy proton detectors](#)

Rev. Sci. Instrum. **79**, 073301 (2008); 10.1063/1.2949388

[Absolute measurements of neutron yields from DD and DT implosions at the OMEGA laser facility using CR-39 track detectors](#)

Rev. Sci. Instrum. **73**, 2597 (2002); 10.1063/1.1487889

Frustrated by old technology? Is your AFM dead and can't be repaired? Sick of bad customer support?



It is time to upgrade your AFM
Minimum \$20,000 trade-in discount
for purchases before August 31st

**Asylum Research is today's
technology leader in AFM**

dropmyoldAFM@oxinst.com

OXFORD
INSTRUMENTS
The Business of Science®

A method for *in situ* absolute DD yield calibration of neutron time-of-flight detectors on OMEGA using CR-39-based proton detectors

C. J. Waugh,^{1,a)} M. J. Rosenberg,² A. B. Zylstra,¹ J. A. Frenje,¹ F. H. Séguin,¹ R. D. Petrasso,¹ V. Yu. Glebov,² T. C. Sangster,² and C. Stoeckl²

¹Plasma Science and Fusion Center, MIT, Cambridge, Massachusetts 02139, USA

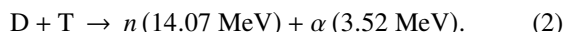
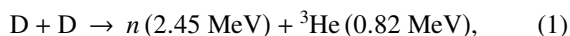
²Laboratory for Laser Energetics, Rochester, New York 14623, USA

(Received 24 January 2015; accepted 16 April 2015; published online 27 May 2015)

Neutron time of flight (nTOF) detectors are used routinely to measure the absolute DD neutron yield at OMEGA. To check the DD yield calibration of these detectors, originally calibrated using indium activation systems, which in turn were cross-calibrated to NOVA nTOF detectors in the early 1990s, a direct *in situ* calibration method using CR-39 range filter proton detectors has been successfully developed. By measuring DD neutron and proton yields from a series of exploding pusher implosions at OMEGA, a yield calibration coefficient of 1.09 ± 0.02 (relative to the previous coefficient) was determined for the 3m nTOF detector. In addition, comparison of these and other shots indicates that significant reduction in charged particle flux anisotropies is achieved when bang time occurs significantly (on the order of 500 ps) after the trailing edge of the laser pulse. This is an important observation as the main source of the yield calibration error is due to particle anisotropies caused by field effects. The results indicate that the CR-39-nTOF *in situ* calibration method can serve as a valuable technique for calibrating and reducing the uncertainty in the DD absolute yield calibration of nTOF detector systems on OMEGA, the National Ignition Facility, and laser megajoule. © 2015 AIP Publishing LLC. [<http://dx.doi.org/10.1063/1.4919290>]

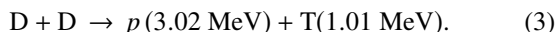
I. INTRODUCTION

On Inertial Confinement Fusion (ICF) facilities such as OMEGA¹ and the National Ignition Facility (NIF),² neutron time-of-flight (nTOF) detectors, operated in current mode, are routinely used to measure parts of the neutron spectrum from which absolute yield,^{3–5} neutron-average ion temperature,^{6–10} bang time (BT),^{11–13} and areal density^{14,15} are inferred. In an ICF implosion, neutrons are mainly generated from the primary fusion reactions in a deuterium (DD), or a deuterium/tritium (DT) fuel mixture,



Historically, for an absolute yield determination, nTOF calibration coefficients were required and obtained by either cross-calibrating to previously calibrated nTOF detectors, or by cross-calibrating to copper (Cu) or indium (In) activation data for DT and DD neutrons, respectively.¹⁶

In this work, a new method for obtaining nTOF DD calibration coefficients has been developed using CR-39 nuclear track detectors.¹⁷ This is done through *in situ* absolute yield measurements of DD protons (DDp) produced in the reaction



Using CR-39 for detection of DDp is ideal for two reasons. First, CR-39 detects DDp with 100% detection efficiency and thus does not need to be calibrated. Second,

the branching ratio of reactions (1) and (3) is nearly unity at plasma conditions relevant to ICF (5–25 keV). An equivalent DDn yield (Y_{DDn}) is therefore easily inferred from the CR-39 DDp yield (Y_{DDp}) using the well-known Y_{DDn}/Y_{DDp} branching ratio. Using this approach for the nTOF absolute yield calibration has the advantage over historic calibration methods in that it removes the systematic errors that are introduced by multiple cross-calibrations between different detectors.

Results from a series of exploding pusher shots at OMEGA confirm that the CR-39-nTOF *in situ* calibration method is a simple and powerful tool for determining calibration coefficients for individual nTOF detectors on OMEGA and that the DD yield calibration component for some of the nTOF detectors on OMEGA should be adjusted. In addition, a comparison of several exploding pusher experiments indicates that significant reduction in charged particle flux anisotropies can be achieved when BT occurs significantly (on the order of 500 ps) after the end of the laser pulse. This is especially noteworthy since a reduction in flux anisotropy reduces the number of CR-39 detectors required for an accurate measurement. This is particularly important on large facilities such as the NIF where diagnostic ports to field CR-39 detectors are limited. We conclude that the method is well suited to reduce the DD calibration uncertainty of nTOF systems on other large ICF facilities such as the NIF^{4,5,18,19} and Laser Megajoule (LMJ).²⁰

This paper is structured as follows. In Sec. II, the CR-39-nTOF *in situ* calibration method is presented along with data taken from two experimental campaigns at OMEGA where the DDn yield from the CR-39 DDp measurement is compared to DDn yield data obtained with 3m nTOF detector to assess the absolute yield calibration of nTOF

^{a)}Author to whom correspondence should be addressed. Electronic mail: cjwaugh@mit.edu

TABLE I. Data used to determine the calibration coefficient and calibration uncertainty of OMEGA 3m nTOF for campaigns A and B. Data consist of CR-39 DDP yields (Y_{DDp}), nTOF DDn yield measurement (Y_{DDn}), nTOF measured plasma ion temperature (T_{iDD}), and associated DDn/DDp branching ratio (β_{np}). The CR-39 detectors were fielded in a trident arrangement in TIM 1-3 and in TIM 5.

Campaign A	Y_{DDp} (10^9)						TIM 5	Y_{DDn} (10^9) (nTOF)	T_{iDD} (keV) (nTOF)	β_{np}
	TIM 1-8:00	TIM 1-12:00	TIM 2-8:00	TIM 2-12:00	TIM 3-8:00	TIM 3-12:00				
64965	5.10	2.44	3.82	3.07	3.81	4.65	5.67	3.42	5.2	0.9873
64967	4.42	3.75	2.96	3.24	4.25	2.62	4.34	3.78	5.3	0.9866
64993	3.24	4.20	3.27	3.95	3.09	2.20	3.99	3.57	5.0	0.9886
64995	6.74	8.41	7.48	7.06	7.02	4.72	3.71	6.13	7.9	0.9708
64997	1.68	1.21	1.10	1.00	1.33	1.50	1.11	1.36	3.8	0.9973
64999	4.65	3.68	3.82	4.02	4.58	4.10	3.91	3.59	4.9	0.9893

Campaign B	Y_{DDp} (10^9)						T5	Y_{DDn} (10^9) (nTOF)	T_{iDD} (keV) (nTOF)	β_{np}
	T1-8:00	T1-12:00	T2-8:00	T2-12:00	T3-8:00	T3-12:00				
64958	4.42	4.55	4.57	4.07	4.60	4.79	3.93	3.95	3.0	1.0037
64961	2.12	2.17	1.89	2.17	2.45	2.32	2.26	1.99	2.9	1.0045
64963	4.12	4.23	3.86	3.81	3.79	3.42	3.40	3.51	2.6	1.0071
65001	1.05	0.97	0.92	0.92	0.97	1.00	0.97	0.90	1.8	1.0147

detectors. In Sec. III, we compare data from a series of experiments and show that a significant reduction in DDP flux anisotropies occurs when BT occurs significantly after the trailing edge of the laser pulse. This is critical to the calibration method described herein. In Sec. IV, we provide an extensive uncertainty analysis that gives a calibration coefficient of 1.09 ± 0.02 relative to the existing OMEGA 3m nTOF calibration coefficient. Section V summarizes this work and discusses the applicability of the method for reducing the uncertainties in the calibration coefficient of nTOF systems on other ICF facilities such as the NIF and LMJ. In Table I, we provide DDP yields determined from individual CR-39 detectors. DDn yields are determined from the 3m nTOF ion temperature and the Y_{DDn}/Y_{DDp} branching ratio at the measured ion temperature.

II. OMEGA nTOF CALIBRATION USING CR-39 DETECTORS

As mentioned, the previous DDn absolute yield calibration coefficient used for the OMEGA nTOF detectors is based on a series of cross-calibrations between particle accelerators, In-activation, and other nTOF detectors with an estimated accuracy of about 10%.⁴³ Here, we consider the possibility of direct calibration to DDP measurements using CR-39 detectors.

A. OMEGA CR-39 measurements of DDP yields

CR-39 detectors are used in a wide array of charged particle and neutron diagnostics on OMEGA and NIF.^{21–29} The CR-39 response to protons, in particular, has been studied extensively and is well documented^{17,30–34} and this work rests on this previous work.

To test the CR-39-nTOF *in situ* calibration method, a series of experiments were conducted at OMEGA where DDn yields obtained from nTOF detectors using the previous calibration coefficient were compared to DDP yields obtained from CR-39 detectors. In these experiments, we used thin-

glass exploding pusher implosions, which produce high ion temperatures and high DDP and DDn yields.

A range filter positioned in front of the CR-39 is made of a single 25 μm thick aluminum foil that filters out low-energy ablator ions and a large fraction of X-rays. Two experimental campaigns were designed and executed to minimize the yield uncertainties in the CR-39 and nTOF measurements. In experimental campaign A, glass capsules nominally 880 μm in diameter, 2.0 μm thick, and filled with 3.6 atm D_2 and 7.9 atm D^3He gas were used. Sixty laser beams providing about 5.2 kJ in a 1-ns square pulse were also used. In experimental campaign B, the capsules were nominally 880 μm in diameter, 2.0 μm thick, and filled with 9.3 atm of D_2 gas. In these experiments, 60 laser beams providing about 2.4 kJ in a 1-ns square wave pulse were used. Smoothing by spectral dispersion (SSD),³⁵ SG4 phase plates, and polarization smoothing³⁶ were applied to both campaigns. An overview of the capsule and laser conditions for both experimental campaigns is given in Fig. 1.

One known issue with measurements of charged-particles from ICF implosions is that large electromagnetic fields are generated around the implosion when the laser is still illuminating the capsules.^{21,37} While this has no effect on

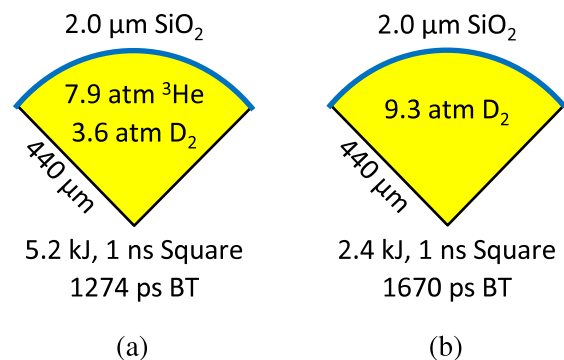


FIG. 1. Nominal target dimensions, gas fill pressures, laser energy and pulse shape, and BT for experimental campaign A (a) and experimental campaign B (b).

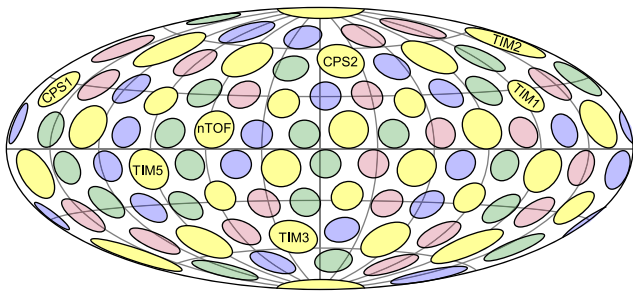


FIG. 2. An Aitoff projection of the OMEGA target chamber showing the diagnostic ports. CR-39 detectors for nTOF calibration campaigns A and B were fielded in ten inch manipulators (TIMs) 1, 2, 3, and 5 to provide broad angular coverage of DDp emissions. The blue, red, and green illustrate ports for the laser beams.

neutrons, the electromagnetic fields deflect charged particles which leads to an anisotropic emission of the charged particles. To average out the effects of electromagnetic field-induced charged-particle flux anisotropies, seven CR-39 detectors were fielded around the implosions to allow broad coverage of the emission. The CR-39 detectors were fielded in standard OMEGA ten inch manipulators (TIMs) using “trident” holders, which allow up to three detectors to be fielded in each TIM. The final configuration included tridents in TIMs 1, 2, and 3, and a single CR-39 detector in TIM 5. All detectors were located 150 cm from the implosion. Location of the TIMs and other diagnostic ports on OMEGA are shown in Fig. 2.

The DDp yields determined from the individual CR-39 measurements in campaigns A and B are given in Fig. 3 along with the OMEGA 3m nTOF DDn yields. The DDp yields from campaign A are on average in close agreement with 3m nTOF measured DDn yields but significant yield variations are observed due to electromagnetic field effects. Yields from campaign B are also in close agreement with the 3m nTOF measured DDn yields, but the variation between measured DDp yields within a given shot is significantly less.

III. RELATION BETWEEN PARTICLE FLUX ANISOTROPIES AND BANG TIME

As can be seen in Fig. 3, the CR-39 data within a shot in campaign A exhibit significantly more yield variation than the

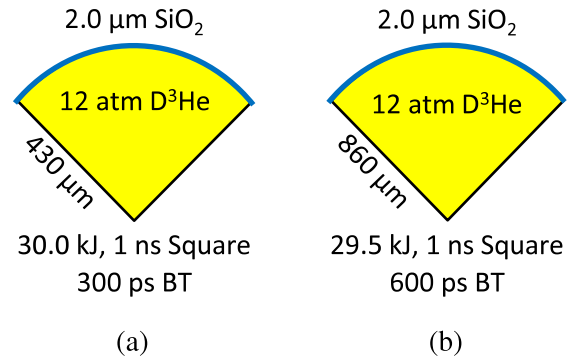


FIG. 4. Nominal target dimensions, gas fill pressures, laser energy and pulse shape, and BT for two experimental designs used in the campaign conducted at OMEGA on January 13, 2012: (a) 430 μm radius and (b) 860 μm radius.

data in campaign B. As noted earlier, the variation between individual yield measurements is not due to measurement error since CR-39 yield measurements have an error of less than 1% but rather are due to electromagnetic fields generated around the capsule implosion.²¹ These fields have been found to be significant when BT occurs while the laser is incident on the capsule. Shots that are designed to have a BT after the trailing edge of the laser pulse produce yields that are insignificantly affected by electromagnetic fields.^{37,38} In general, BT scales inversely with laser energy or power. The BT is also affected by the capsule material, shell thickness, and diameter. In Fig. 5, we present the yield variation as a function of BT for four exploding pusher campaigns. The 1-ns square laser pulse used in these experiments is also illustrated for comparison. As can be seen, significant yield variations are observed in the January 13, 2012 campaign when BT occurred early or in the middle of the pulse. In contrast, the yield variations are very small in campaign B when BT on average occurred approximately 500 ps after the laser turned off. The two experimental designs that were used for the January 13, 2012 campaign are given in Fig. 4.

By comparing these different campaigns, we conclude that exploding pusher shots with lower energy laser drives can be designed to have BTs after the laser shuts off, which results in less yield variation and less uncertainty in the overall yield measurement.

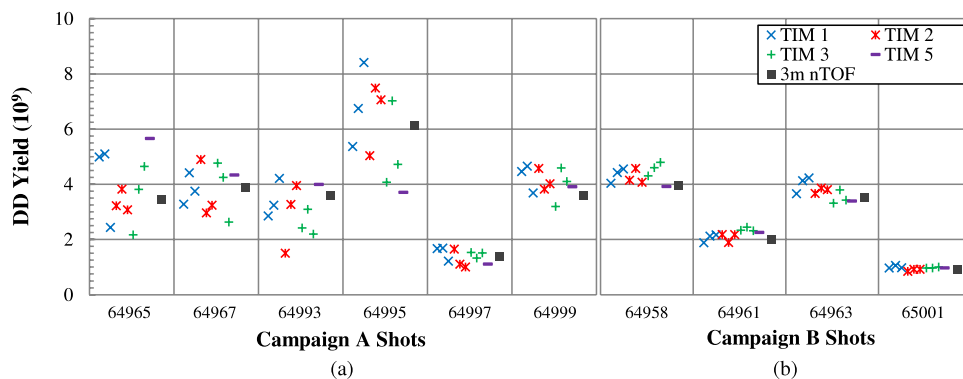


FIG. 3. Measured DDp yields using CR-39 detectors positioned in TIMs 1, 2, 3, and 5, and measured DDn yield using 3m nTOF for (a) campaign A and (b) campaign B shots. The DDp yields measured in campaign A display significant variation due to electromagnetic fields around the implosion, whereas the DDp yields measured in campaign B display very little spread. The CR-39 measured DDp yields are in good agreement with DDn yields measured by 3m nTOF.

IV. CR-39-nTOF YIELD COMPARISON AND CALIBRATION COEFFICIENT DETERMINATION

When determining the 3m nTOF calibration coefficient, uncertainties associated with the CR-39 DDp yield measurement, the nTOF DDn yield measurement, and the DDn/DDp branching ratio are taken into account. Uncertainties associated with the CR-39 DDp yield measurement largely come from three sources: (1) statistical uncertainty associated with the number of counts, (2) uncertainty associated with the signal to background level, and most importantly (3) uncertainty in overall yield due to electromagnetic field-induced charged particle anisotropies. As the number of recorded tracks on a CR-39 detector was between 8×10^3 and 8×10^4 , counting statistics result in uncertainties less than 1% and can therefore be neglected. In the software used to analyze CR-39 data, background is separated from signal by differentiating tracks based on size, eccentricity, and contrast.¹⁷ Using track differentiating techniques, signal to background separation generally results in only a few percent uncertainty. With statistical and signal to background separation uncertainties less than a few percent, the uncertainties stemming from electromagnetic-field-induced particle-flux anisotropies tend to dominate. As has been stated, these uncertainties, typically 5-10%, are reduced by increasing the number of CR-39 detectors fielded around the implosion to get better coverage and by designing shots to generate a BT that occurs after the end of the laser pulse as shown in Fig. 5.

Uncertainty of the nTOF measurement and its calibration coefficient consists of the uncertainty in the nTOF neutron response, cable reflections, and noise. The uncertainty in the nTOF instrument response is estimated to be about 5%.⁴³

The DDn/DDp branching ratio depends on the reactivity of the two reaction branches and is near unity for the relevant temperatures (2-8 keV).³⁹⁻⁴¹ Instead of assuming the ratio to be unity in the analysis, we use the measured fuel burn-average ion temperatures obtained from nTOF to calculate values of the branching ratio from the parametrization of the DDn and DDp reactivities found in Bosch and Hale.⁴⁰ The uncertainty in the nTOF ion temperature is around 10%⁴² and the uncertainty in the Bosch and Hale parametrization is $\ll 1\%$. For the measured ion temperatures obtained in campaigns A and B,

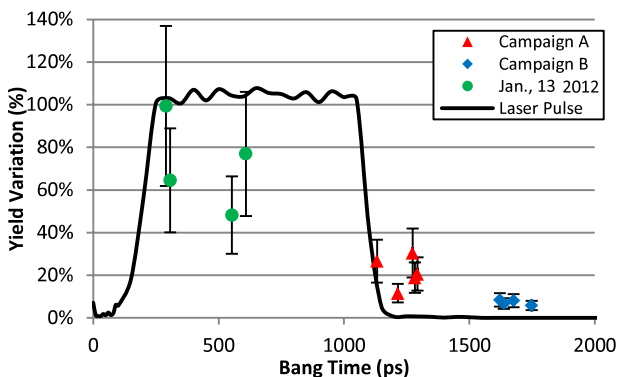


FIG. 5. Yield variation as a function of bang time for four exploding pusher campaigns. The laser pulse used in these experiments is also illustrated for comparison. Significant yield variations are observed when bang time occurs during the laser pulse. In contrast, the yield variations are smaller when bang times occurs after the laser pulse.

the calculated branching ratios lie between 1.0147 ± 0.0091 and 0.9708 ± 0.0220 . (See Table I for all calculated branching ratios.)

Using the DDn/DDp branching ratio and the CR-39 measured DDp yield (Y_{DDp}), an equivalent DDn yield measurement (Y_{CR-39n}) is obtained. The ratio of each Y_{CR-39n} to the nTOF DDn yield (Y_{nTOF}) is then determined. In the absence of electromagnetic-field effects and assuming the nTOF calibration coefficient is perfectly calibrated, the expected value of Y_{CR-39n}/Y_{nTOF} for each measurement is unity. Any shot specific phenomena that would affect the DDp yield should also affect the DDn yield such that the expected values would be equal provided the correct branching ratio is used. In practice, field effects are present so that the value of Y_{CR-39n}/Y_{nTOF} for individual measurements is rarely unity, especially when BT occurs during the laser pulse (which as noted results in anisotropic particle emissions and large yield variation among CR-39 detector measurements). In the case where BT occurs after the laser pulse, field effects are much smaller and Y_{CR-39n}/Y_{nTOF} is typically close to unity for each individual measurement. However, by taking an average of all Y_{CR-39n} values on a given shot, field effects are mostly averaged out, resulting in a better determination of the overall yield. By averaging out field effects, the effect of the existing nTOF calibration coefficient can be assessed. Any statistically significant deviation from unity would suggest an anomaly in the existing calibration coefficient. The expected ratio obtained by averaging out field effects over a series of CR-39 detectors and shots can be expressed as

$$\left\langle \frac{Y_{CR-39n}}{Y_{nTOF}} \right\rangle = \frac{1}{n} \sum_{Shot,i} \sum_{CR-39,j} \frac{Y_{DDp}(i,j) \cdot \beta_{np}(i)}{Y_{DDn}(i)}, \quad (4)$$

where Y_{CR-39n} is the DDn yield inferred from the CR-39 DDp measurement, Y_{nTOF} is the nTOF measured DDn yield, $Y_{DDp}(i,j)$ is the CR-39 DDp measurement for shot i and CR-39 detector j , $\beta_{np}(i)$ is the DDn/DDp branching ratio for shot i , $Y_{DDn}(i)$ is the DDn nTOF measurement for shot i , and n is the total number of CR-39 DDp measurements taken over all shots ($i \times j$). Individual DDp CR-39 yield measurements, 3m nTOF DDn yield measurements, nTOF measured plasma ion temperature and calculated DDn/DDp branching ratio are given in Table I.

While the effect of the calibration coefficient for the 3m nTOF can be isolated by averaging out field effects, determining whether any deviation from an expected value of unity is statistically significant requires the evaluation of the uncertainties associated with the CR-39 DDp measurement, DDn/DDp branching ratio, nTOF DDn measurement, and yield variation. The two sources of error are instrumental (σ_E)

TABLE II. The errors associated with the average Y_{CR-39n}/Y_{nTOF} ratios obtained in campaign A and campaign B. σ_E is the combined instrumental error, σ_C is the error from yield variation (due predominantly to field effects), and σ_{Tot} is the total error.

Shots	σ_E	σ_C	σ_{Tot}
Campaign A	0.011	0.037	0.038
Campaign B	0.012	0.014	0.019

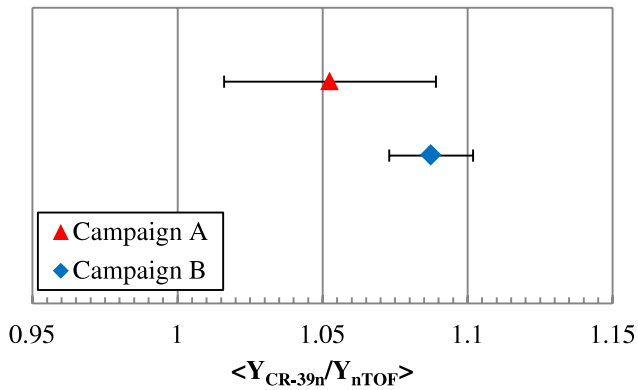


FIG. 6. The expected value of the average of the inferred CR-39 to nTOF DDn yield ratio ($\langle Y_{CR-39n}/Y_{nTOF} \rangle$) determined from data obtained in the two experimental campaigns. In campaign A, the bang time occurred close to the end of the laser pulse, while in campaign B, bang time occurred well after the trailing edge of the laser pulse.

and yield variation due to field effects (σ_C). σ_E is determined by propagating the errors associated with Y_{DDp} , Y_{DDn} and β_{np} in accordance with Eq. (4) to produce an overall instrumental error. Here, we assume Y_{CR-39n} and Y_{nTOF} to be perfectly correlated, as an increase in the yield of protons should track the neutron yield and vice versa. σ_C is determined in the usual way as the standard deviation of Y_{CR-39n}/Y_{nTOF} divided by \sqrt{n} . The total error is obtained by adding σ_E to σ_C in quadrature, as given in

$$\sigma_{Tot}^2 = \sigma_C^2 + \sigma_E^2. \quad (5)$$

If the instrumental uncertainty is small ($\sigma_C \gg \sigma_E$), then the overall uncertainty is just the uncertainty associated with the spread of individual Y_{CR-39n}/Y_{nTOF} ratios, which is almost entirely driven by field effects. The instrumentation error (σ_E), yield-variation error (σ_C), and total error (σ_{Tot}) for campaigns A and B are given in Table II.

As can be seen in Table II, the uncertainty in the DDp measurement that arises from electromagnetic field effects dominates the instrumental error. In Fig. 6, the determined ratios from the data obtained in campaigns A and B are shown. From this plot, one observes that the greater yield spread in campaign A than in campaign B has a significant effect on the total error. Since the total error in campaign A is dominated by field effects, and since the CR-39 DDp measurements in campaign B have less yield variation, the campaign B calibration is more accurate. Using campaign B data, we calculate the 3m nTOF DDn calibration coefficient to be 1.09 ± 0.02 . This confirms that the 3m nTOF DD calibration coefficient is within the estimated 10% uncertainty range, but may be low by $9\% \pm 2\%$.

V. CONCLUSION

In conclusion, a new method for obtaining DDn nTOF absolute yield calibration coefficients through *in situ* measurements of DDp yields has successfully been implemented at OMEGA. The method involves calibration of nTOF measurements using DDp measured with a CR-39 detector. From the DDp yield, the CR-39 inferred DDn yield is determined through the well-known Y_{DDn}/Y_{DDp} branching

ratio. The advantage of this approach is that it removes the systematic errors associated with the several cross-calibrations between accelerators, In-activation systems, and other nTOF detectors that had previously been used to calibrate OMEGA 3m nTOF.

Results from a series of exploding pusher campaigns at OMEGA confirms that the 3m nTOF DD calibration coefficient is within the estimated 10% uncertainty range, but may be low by $9\% \pm 2\%$. It has also been shown that the uncertainty in the calibration coefficient obtained in this work is mainly due to electromagnetic-field-induced charge particle flux anisotropies and not instrumentation error. To minimize this effect, implosions were designed to generate a bang time well after the trailing edge of the laser pulse. The CR-39/nTOF *in situ* calibration method is a simple yet powerful technique for DD yield calibration of individual nTOF detectors on OMEGA. Due to its simplicity, this method can be easily transferred to calibrate nTOF systems on other large ICF facilities such as the NIF^{4,5,18,19} and LMJ.²⁰

ACKNOWLEDGMENTS

The authors acknowledge and thank the engineering, operations, and technical staff at the Laboratory for Laser Energetics (LLE), as well as E. Doeg and R. Frankel (MIT) and M. Burke (LLE) for a significant effort preparing and processing CR-39.

This work was done in part for C. J. Waugh's S.M thesis and was supported in part by the U.S. Department of Energy (DOE) (No. DE-FG52-09NA-29553), the National Laser User's Facility (DOE Award No. DE-NA0000877), the Fusion Science Center at the University of Rochester (Rochester Sub Award PO No. 415023-G), and the Laboratory for Laser Energetics (LLE) (No. 412160-001G).

¹T. R. Boehly, D. L. Brown, R. S. Craxton, R. L. Keck, J. P. Knauer, J. H. Kelly, T. J. Kessler, S. A. Kumpan, S. J. Loucks, S. A. Letzring, F. J. Marshall, R. L. McCrory, S. F. B. Morse, W. Seka, J. M. Soures, and C. P. Verdon, *Opt. Commun.* **133**, 495 (1997).

²G. H. Miller, E. I. Moses, and C. R. Wuest, *Nucl. Fusion* **44**, S228 (2004).

³M. D. Cable and M. B. Nelson, *Rev. Sci. Instrum.* **59**, 1738 (1988).

⁴V. Glebov, C. Stoeckl, T. Sangster, S. Roberts, G. Schmid, R. Lerche, and M. Moran, *Rev. Sci. Instrum.* **75**, 3559 (2004).

⁵V. Y. Glebov, T. C. Sangster, C. Stoeckl, J. P. Knauer, W. Theobald, K. L. Marshall, M. J. Shoup III, T. Buczek, M. Cruz, T. Duffy, M. Romanofsky, M. Fox, A. Pruyne, M. J. Moran, R. A. Lerche, J. McNaney, J. D. Kilkenny, M. J. Eckart, D. Schneider, D. Munro, W. Stoeffl, R. Zacharias, J. J. Haslam, T. Clancy, M. Yeoman, D. Warwas, C. J. Horsfield, J.-L. Bourgade, O. Landoas, L. Disdier, G. A. Chandler, and R. J. Leeper, *Rev. Sci. Instrum.* **81**, 10D325 (2010).

⁶R. A. Lerche, L. W. Coleman, J. W. Houghton, D. R. Speck, and E. K. Storm, *Appl. Phys. Lett.* **31**, 645 (1977).

⁷R. A. Lerche and B. A. Remington, *Rev. Sci. Instrum.* **61**, 3131 (1990).

⁸M. A. Rusotto and R. L. Kremens, *Rev. Sci. Instrum.* **61**, 3125 (1990).

⁹T. J. Murphy and R. A. Lerche, *Rev. Sci. Instrum.* **63**, 4883 (1992).

¹⁰T. J. Murphy, R. A. Lerche, C. Bennett, and G. Howe, *Rev. Sci. Instrum.* **66**, 930 (1995).

¹¹C. Stoeckl, V. Y. Glebov, J. Zuegel, D. Meyerhofer, and R. Lerche, *Rev. Sci. Instrum.* **73**, 3796 (2002).

¹²V. Y. Glebov, C. Stoeckl, T. Sangster, C. Mileham, S. Roberts, and R. Lerche, *Rev. Sci. Instrum.* **77**, 10E712 (2006).

¹³R. A. Lerche, D. R. Kania, S. M. Lane, G. L. Tietbohl, C. K. Bennett, and G. P. Baltzer, *Rev. Sci. Instrum.* **59**, 1697 (1988).

¹⁴V. Y. Glebov, C. J. Forrest, K. L. Marshall, M. Romanofsky, T. C. Sangster, M. J. Shoup, and C. Stoeckl, *Rev. Sci. Instrum.* **85**, 11E102 (2014).

- ¹⁵C. Forrest, P. Radha, V. Y. Glebov, V. Goncharov, J. Knauer, A. Pruynne, M. Romanofsky, T. Sangster, M. Shoup III, C. Stoeckl *et al.*, *Rev. Sci. Instrum.* **83**, 10D919 (2012).
- ¹⁶C. L. Ruiz, R. J. Leeper, F. A. Schmidlapp, G. Cooper, and D. J. Malbrough, *Rev. Sci. Instrum.* **63**, 4889 (1992).
- ¹⁷F. H. Seguin, J. A. Frenje, C. K. Li, D. G. Hicks, S. Kurebayashi, J. R. Rygg, B. E. Schwartz, R. D. Petrasso, S. Roberts, J. M. Soares, D. D. Meyerhofer, T. C. Sangster, J. P. Knauer, C. Sorce, V. Y. Glebov, C. Stoeckl, T. W. Phillips, R. J. Leeper, K. Fletcher, and S. Padalino, *Rev. Sci. Instrum.* **74**, 975 (2003).
- ¹⁸R. A. Lerche, V. Y. Glebov, M. J. Moran, J. M. McNaney, J. D. Kilkenny, M. J. Eckart, R. A. Zacharias, J. J. Haslam, T. J. Clancy, M. F. Yeoman, D. P. Warwas, T. C. Sangster, C. Stoeckl, J. P. Knauer, and C. J. Horsfield, *Rev. Sci. Instrum.* **81**, 10D319 (2010).
- ¹⁹Z. Ali, V. Glebov, M. Cruz, T. Duffy, C. Stoeckl, S. Roberts, T. Sangster, R. Tommasini, A. Throop, and M. Moran, *Rev. Sci. Instrum.* **79**, 10E527 (2008).
- ²⁰O. Landoas, V. Y. Glebov, B. Rosse, M. Briat, L. Disdier, T. C. Sangster, T. Duffy, J. G. Marmouget, C. Varignon, X. Ledoux, T. Caillaud, I. Thfoin, and J.-L. Bourgade, *Rev. Sci. Instrum.* **82**, 073501 (2011).
- ²¹J. R. Rygg, F. H. Séguin, C. K. Li, J. A. Frenje, M. J.-E. Manuel, R. D. Petrasso, R. Betti, J. A. Delettrez, O. V. Gotchev, J. P. Knauer, D. D. Meyerhofer, F. J. Marshall, C. Stoeckl, and W. Theobald, *Science* **319**, 1223 (2008).
- ²²D. T. Casey, J. A. Frenje, M. G. Johnson, F. H. Seguin, C. K. Li, R. D. Petrasso, V. Y. Glebov, J. Katz, J. P. Knauer, D. D. Meyerhofer, T. C. Sangster, R. M. Bionta, D. L. Bleuel, T. Doppner, S. Glenzer, E. Hartouni, S. P. Hatchett, S. Le Pape, T. Ma, A. MacKinnon, M. A. McKernan, M. Moran, E. Moses, H. S. Park, J. Ralph, B. A. Remington, V. Smalyuk, C. B. Yeaman, J. Kline, G. Kyrala, G. A. Chandler, R. J. Leeper, C. L. Ruiz, G. W. Cooper, A. J. Nelson, K. Fletcher, J. Kilkenny, M. Farrell, D. Jasion, and R. Paguio, *Rev. Sci. Instrum.* **83**, 10D912 (2012).
- ²³F. H. Seguin, N. Sinenian, M. Rosenberg, A. Zylstra, M. J. E. Manuel, H. Sio, C. Waugh, H. G. Rinderknecht, M. G. Johnson, J. Frenje, C. K. Li, R. Petrasso, T. C. Sangster, and S. Roberts, *Rev. Sci. Instrum.* **83**, 10D908 (2012).
- ²⁴M. J. E. Manuel, A. B. Zylstra, H. G. Rinderknecht, D. T. Casey, M. J. Rosenberg, N. Sinenian, C. K. Li, J. A. Frenje, F. H. Seguin, and R. D. Petrasso, *Rev. Sci. Instrum.* **83**, 063506 (2012).
- ²⁵A. B. Zylstra, J. A. Frenje, F. H. Seguin, M. J. Rosenberg, H. G. Rinderknecht, M. G. Johnson, D. T. Casey, N. Sinenian, M. J. E. Manuel, C. J. Waugh, H. W. Sio, C. K. Li, R. D. Petrasso, S. Friedrich, K. Knittel, R. Bionta, M. McKernan, D. Callahan, G. W. Collins, E. Dewald, T. Doppner, M. J. Edwards, S. Glenzer, D. G. Hicks, O. L. Landen, R. London, A. Mackinnon, N. Meezan, R. R. Prasad, J. Ralph, M. Richardson, J. R. Rygg, S. Sepke, S. Weber, R. Zacharias, E. Moses, J. Kilkenny, A. Nikroo, T. C. Sangster, V. Glebov, C. Stoeckl, R. Olson, R. J. Leeper, J. Kline, G. Kyrala, and D. Wilson, *Rev. Sci. Instrum.* **83**, 10D901 (2012).
- ²⁶A. B. Zylstra, C. K. Li, H. G. Rinderknecht, F. H. Seguin, R. D. Petrasso, C. Stoeckl, D. D. Meyerhofer, P. Nilson, T. C. Sangster, S. Le Pape, A. Mackinnon, and P. Patel, *Rev. Sci. Instrum.* **83**, 013511 (2012).
- ²⁷J. A. Frenje, D. T. Casey, C. K. Li, J. R. Rygg, F. H. Seguin, R. D. Petrasso, V. Y. Glebov, D. D. Meyerhofer, T. C. Sangster, S. Hatchett, S. Haan, C. Cerjan, O. Landen, M. Moran, P. Song, D. C. Wilson, and R. J. Leeper, *Rev. Sci. Instrum.* **79**, 10E502 (2008).
- ²⁸C. K. Li, F. H. Seguin, J. A. Frenje, J. R. Rygg, R. D. Petrasso, R. P. J. Town, P. A. Amendt, S. P. Hatchett, O. L. Landen, A. J. Mackinnon, P. K. Patel, V. A. Smalyuk, J. P. Knauer, T. C. Sangster, and C. Stoeckl, *Rev. Sci. Instrum.* **77**, 10E725 (2006).
- ²⁹J. A. Frenje, K. M. Green, D. G. Hicks, C. K. Li, F. H. Seguin, R. D. Petrasso, T. C. Sangster, T. W. Phillips, V. Y. Glebov, D. D. Meyerhofer, S. Roberts, J. M. Soares, C. Stoeckl, K. Fletcher, S. Padalino, and R. J. Leeper, *Rev. Sci. Instrum.* **72**, 854 (2001).
- ³⁰N. Sinenian, M. J. Rosenberg, M. Manuel, S. C. McDuffee, D. T. Casey, A. B. Zylstra, H. G. Rinderknecht, M. G. Johnson, F. H. Seguin, J. A. Frenje, C. K. Li, and R. D. Petrasso, *Rev. Sci. Instrum.* **82**, 103303 (2011).
- ³¹M. J. E. Manuel, M. J. Rosenberg, N. Sinenian, H. Rinderknecht, A. B. Zylstra, F. H. Seguin, J. Frenje, C. K. Li, and R. D. Petrasso, *Rev. Sci. Instrum.* **82**, 095110 (2011).
- ³²D. T. Casey, J. A. Frenje, F. H. Seguin, C. K. Li, M. J. Rosenberg, H. Rinderknecht, M. J. E. Manuel, M. G. Johnson, J. C. Schaeffer, R. Frankel, N. Sinenian, R. A. Childs, R. D. Petrasso, V. Y. Glebov, T. C. Sangster, M. Burke, and S. Roberts, *Rev. Sci. Instrum.* **82**, 073502 (2011).
- ³³A. B. Zylstra, H. G. Rinderknecht, N. Sinenian, M. J. Rosenberg, M. Manuel, F. H. Seguin, D. T. Casey, J. A. Frenje, C. K. Li, and R. D. Petrasso, *Rev. Sci. Instrum.* **82**, 083301 (2011).
- ³⁴A. B. Zylstra, J. A. Frenje, F. H. Séguin, M. Gatou Johnson, D. T. Casey, M. J. Rosenberg, C. Waugh, N. Sinenian, M. J. E. Manuel, C. K. Li, R. D. Petrasso, Y. Kim, and H. W. Herrmann, *Nucl. Instrum. Methods Phys. Res., Sect. A* **681**, 84 (2012).
- ³⁵S. P. Regan, J. A. Marozas, J. H. Kelly, T. R. Boehly, W. R. Donaldson, P. A. Jaanimagi, R. L. Keck, T. J. Kessler, D. D. Meyerhofer, W. Seka, S. Skupsky, and V. A. Smalyuk, *J. Opt. Soc. Am. B* **17**, 1483 (2000).
- ³⁶T. R. Boehly, V. A. Smalyuk, D. D. Meyerhofer, J. P. Knauer, D. K. Bradley, R. S. Craxton, M. J. Guardalben, S. Skupsky, and T. J. Kessler, *J. Appl. Phys.* **85**, 3444 (1999).
- ³⁷D. G. Hicks, C. K. Li, F. H. Séguin, A. K. Ram, J. A. Frenje, R. D. Petrasso, J. M. Soares, V. Y. Glebov, D. D. Meyerhofer, S. Roberts, C. Sorce, C. Stöckl, T. C. Sangster, and T. W. Phillips, *Phys. Plasmas* **7**, 5106 (2000).
- ³⁸N. Sinenian, A. B. Zylstra, M. J.-E. Manuel, H. G. Rinderknecht, J. A. Frenje, F. H. Séguin, C. K. Li, R. D. Petrasso, V. Goncharov, J. Delettrez, I. V. Igumenshchev, D. H. Froula, C. Stoeckl, T. C. Sangster, D. D. Meyerhofer, J. A. Cobble, and D. G. Hicks, *Appl. Phys. Lett.* **101**, 114102 (2012).
- ³⁹A. Boughrara, H. Beaumevielle, and S. Ouichaoui, *Europhys. Lett.* **48**, 264 (1999).
- ⁴⁰H.-S. Bosch and G. Hale, *Nucl. Fusion* **32**, 611 (1992).
- ⁴¹M. Erba, *J. Phys. D: Appl. Phys.* **27**, 1874 (1994).
- ⁴²V. Y. Glebov, C. Stoeckl, T. C. Sangster, C. J. Forrest, and R. A. Lerch, *Bull. Am. Phys. Soc.* **57**, 12 (2012).
- ⁴³V. Y. Glebov, private communication (2014).